Journal of Dental Sciences 21 (2026) 115–124

Available online at www.sciencedirect.com

ScienceDirect

journal homepage: www.e-jds.com

Original Article

Suppression of distal-less homeobox 3 increased alveolar bone mass in mouse tooth socket by targeting thrombospondin 1

Chang Diao [a†], Fang Li [b†], Kai Sun [a], Miao Yu [a], Haochen Liu [a], Hailan Feng [a], Yang Liu [a**], Dong Han [a*]

[a] *Department of Prosthodontics, Peking University School and Hospital of Stomatology, National Center for Stomatology, National Clinical Research Center for Oral Diseases, National Engineering Research Center of Oral Biomaterials and Digital Medical Devices, China*

[b] *Third Clinical Division, Peking University School and Hospital of Stomatology, National Center for Stomatology, National Clinical Research Center for Oral Diseases, National Engineering Research Center of Oral Biomaterials and Digital Medical Devices, China*

Received 19 June 2025; Final revision received 7 July 2025
Available online 23 July 2025

KEYWORDS
Alveolar bone remodeling;
Dlx3;
Gene therapy;
Thbs1

Abstract *Background/purpose:* Alveolar ridge resorption after tooth extraction significantly impacts dental implantation and prosthodontic treatment outcomes. Sustaining alveolar bone mass remains a critical clinical challenge and a major focus of research. Notably, patients with tricho-dento-osseous (TDO) syndrome, characterized by distal-less homeobox 3(*DLX3*) loss-of function mutations, exhibit increased jaw bone density and demonstrate long-term preservation of alveolar bone mass post-tooth extraction. This study aimed to investigate the effects of *DLX3* knockdown on bone remodeling following tooth extraction and to elucidate the underlying molecular mechanisms.

Materials and methods: we established a murine maxillary incisor extraction model to investigate alveolar bone healing. An empty adenoviral vector or an adenoviral vector designed to suppress *Dlx3* gene expression was delivered into the alveolar sockets of wild-type C57BL/6 mice, respectively. Histological staining, micro-computed tomography (micro-CT), immunohistochemistry, immunofluorescence, and RNA sequencing were employed to evaluate the outcomes.

Results: Histological analysis revealed accelerated bone formation and increased alveolar bone mass in the *Dlx3*-knockdown group. This phenotype was attributed to the activation of

* Corresponding author. Department of Prosthodontics, Peking University School and Hospital of Stomatology, No. 22, Zhongguancun South Avenue, Haidian District, Beijing 100081, China.

** Corresponding author. Department of Prosthodontics, Peking University School and Hospital of Stomatology, No. 22, Zhongguancun South Avenue, Haidian District, Beijing 100081, China.

E-mail addresses: pkussliuyang@bjmu.edu.cn (Y. Liu), donghan@bjmu.edu.cn (D. Han).

† These authors contributed equally to this work.

https://doi.org/10.1016/j.jds.2025.07.008

osteoblasts, which promoted new bone formation, and the inhibition of osteoclasts, which reduced bone resorption, without compromising normal bone structure of newly formed bone. RNA sequencing identified thrombospondin 1(*Thbs1*) as a key downstream gene. Downregulation of *Thbs1* following *Dlx3*-knockdown enhanced angiogenesis and osteogenesis. Conversely, the addition of recombinant THBS1 protein after *Dlx3* inhibition partially reversed the enhanced osteogenic phenotype.

Conclusion: Suppression of *Dlx3* increased alveolar bone mass by down-regulation of *Thbs1*. Our study provides a theoretical foundation for developing novel strategies to preserve alveolar bone.

Introduction

The alveolar bone undergoes continuous resorption after tooth extraction, leading to reductions in both height and width. This bone loss complicates subsequent restorative procedures, such as dental implantation and conventional prosthodontic treatments, ultimately affecting both aesthetics and function. To address this issue, several methods have been developed, with the primary clinical approach being bone grafting. Bone grafting utilizes autogenous, allogenic, or xenogeneic bone substitutes to fill the defect and promote integration with the existing bone.[1,2] However, these approaches have significant limitations, including the need for additional donor sites, the risk of graft resorption or integration failure, and potential infections.[3,4] Ongoing research focuses on novel biomaterials and advanced manufacturing techniques.[5,6] One emerging strategy is gene therapy, which involves transferring genetic material into host cells using viral or non-viral vectors to modulate gene expression in target cells, such as osteoblasts, thereby enhancing bone regeneration. This technique offers a promising alternative by enabling the sustained production of physiological growth factors.[7,8]

Following tooth extraction, human sockets initially fill with a fibrin-rich clot that transitions into vascularized granulation tissue containing mesenchymal cells and leukocytes. As healing progresses, leukocyte infiltration diminishes while collagen deposition increases, forming provisional connective tissue. This matrix subsequently develops woven bone, which undergoes remodeling into mature lamellar bone and marrow space.[9,10] In mice, alveolar bone healing post-tooth extraction follows a similar sequence.[11,12] The healing process of alveolar bone involves dynamic interactions between osteogenesis and osteolysis, including the coupling of osteogenesis and angiogenesis.[11]

Distal-less homeobox 3(*DLX3*) has been less extensively investigated in dental biology. As a member of the distal-less transcription factor family,[13] *DLX3* plays a critical role in the development of various organs, including teeth, and bone.[14–16] Mutations in *DLX3* are associated with Tricho-dento-osseous syndrome (TDO syndrome, OMIM #190320),[17] a rare autosomal dominant disorder characterized by abnormal ectodermal organ development. Clinical manifestations include hypoplastic enamel and dentin, and increased skull and jawbone density.[18–20] Given its pivotal role in bone development, *DLX3* has garnered attention as a potential modulator of bone regeneration in the alveolar bone. Patients with *DLX3*-mutated TDO syndrome experience significantly less alveolar bone loss after tooth extraction than normal individuals, facilitating subsequent restorative procedures.While *Dlx3* transgenic mice display increased bone density, they exhibit severe systemic phenotypes.[21,22] Previous studies on *Dlx3* transgenic models have primarily focused on long bones, and the long-term outcomes of osteogenesis and osteolysis. In contrast, alveolar bone defects, such as those caused by tooth extraction or inflammatory lesions, involve relatively short-term remodeling processes.[23] The objective of this study was to use a mouse incisor-extraction model to explore whether transient and localized inhibition of *Dlx3* in the alveolar socket could enhance alveolar bone mass without inducing side effects. This approach holds significant clinical potential in dental practice and addresses a novel issue in alveolar bone research.

This study investigated the role of *Dlx3* in mouse alveolar bone remodeling and elucidated the underlying mechanisms. Our findings indicated that *DLX3* is a promising therapeutic target for enhancing alveolar bone regeneration post-tooth extraction.

Materials and methods

Adenoviral vectors

The *Dlx3* small interfering RNAs (siRNAs), using an adenoviral vector (Ad-*Dlx3*-knockdown), were designed and synthesized by Beijing Likeli Biotechnology(Beijing, China). Adenovirus, transfected with control green fluorescent protein (GFP), served as a control (Ad-Control). Infection efficiency and duration were assessed by detecting GFP signals using inverted fluorescence microscopy; adenovirus knockdown efficacy was confirmed by Western blotting (see Supplementary Information).

Animal and surgical protocol

Twelve-week-old C57BL/6 mice from Peking University Health Science Center's Zoology Department were anesthetized with sodium pentobarbital (50 mg/kg

intraperitoneally) under protocols approved by the Institutional Animal Ethics Committee (LA2019333). The maxillary right incisor was extracted, and the root segments were loosened with a modified dental explorer before being removed using tweezers. The procedure was performed carefully to avoid tooth fracture; otherwise, the animal would be excluded from the study.[5] Mice were divided into two groups: Ad-Control received Ad-GFP-soaked gelatin sponges, and Ad-*Dlx3*-knockdown received Ad-GFP-sh*Dlx3*-soaked sponges, implanted into extraction sockets. Maxillae were ultimately collected. For phenotypic reversal assays, Ad-*Dlx3*-knockdown mice received intra-socket implants of NS(normal saline)-soaked or THBS1-soaked gelatin sponges on postoperative day two.

Hematoxylin and eosin staining, tartrate-resistant acid phosphatase staining, immunohistochemical analysis, and immunofluorescence assays

Samples were fixed in 4 % paraformaldehyde for 24 h, decalcified in 10 % EDTA for 14 days, and paraffin-embedded. Sections were stained with hematoxylin and eosin (H&E) or tartrate-resistant acid phosphatase (TRAP) according to manufacturer protocols and imaged using an Olympus BX51 microscope (Olympus, Tokyo, Japan). For immunohistochemistry(IHC), deparaffinized sections underwent endogenous peroxidase blockade (3 % H_2O_2, 10 min) and blocking with 5 % goat serum (ZSGB-BIO, Beijing, China), followed by overnight incubation at 4 °C with primary antibodies: anti-runt-related transcription factor 2 (RUNX2) (1:100; Proteintech, #20700-1-AP, Chicago, IL, USA) and anti-THBS1 (1:100; Proteintech, #18304-1-AP). After PBS washes, sections were incubated with HRP-conjugated goat anti-rabbit IgG (ZSGB-BIO) and developed with a DAB kit (ZSGB-BIO). For immunofluorescence(IF), antigen-retrieved sections were blocked (1h, RT) and incubated with anti-Endomucin (EMCN; 1:100, #14-5851-81, Invitrogen, Carlsbad, CA, USA), followed by secondary antibodies (ZSGB-BIO) and DAPI counterstaining (Solarbio, Beijing, China). All imaging used the Olympus BX51 system.

Micro-computed tomography analysis

Three weeks post-surgery, mice were euthanized and maxillae fixed in 4 % paraformaldehyde at room temperature for 24 h. Then they were scanned using an Inveon MM system (Siemens, Munich, Germany) to observe the morphology of the root furcation. Images were obtained at 80 kV (voltage), 500 μA (current), 10 μm (pixel size), and 1500 ms (exposure time for each 360 rotational steps). Images were captured using the Inveon MM software. Within the alveolar socket's coronal third, a cylindrical region of interest(ROI) was defined for trabecular quantification, including bone volume (Tb.BV), bone volume fraction (BV/TV), bone surface (Tb.BS), trabecular separation (Tb.Sp), and trabecular number (Tb.N).

RNA sequencing analysis

Three biological replicates of RNA samples from the Ad-Control group mice and five biological replicates from the Ad-*Dlx3*-knockdown group mice, derived from the alveolar bone, were collected five days after surgery. mRNA extraction, cDNA library construction, and sequencing using the BGISEQ 500 sequencing system were performed by BGI (Shenzhen, China). The raw sequence data underwent trimming and quality evaluation using SOAPnuke (https://github.com/BGI-flexlab/SOAPnuke). Subsequently, the clean reads were aligned to the reference genome using HISAT2 (http://ccb.jhu.edu/software/hisat), ensuring accurate mapping of the transcripts. RSEM (http://deweylab.biostat.wisc.edu/rsem) was used to calculate the gene expression levels of each sample. Differentially expressed genes (DEGs) were identified using the DESeq2 statistical method. The DEGs were further analyzed using the Dr-TOM online analysis tool (http://report.bgi.com) with the Kyoto Encyclopedia of Genes and Genomes (KEGG) and Gene Ontology (GO) databases.

Statistical analysis

Quantitative data are expressed as the mean ± standard deviation (SD). Statistical analyses were performed using the SPSS version 27.0 software package (IBM SPSS Inc, Chicago, IL, USA). The data were analyzed using the Student's t-test, and a *P*-value <0.05 was considered statistically significant.

Results

Construction of mouse model with temporary *Dlx3*-inhibition in tooth extraction sockets

The right upper incisors were extracted from 12-week-old C57BL/6 mice, with adenovirus-loaded gelatin sponges implanted into sockets to inhibit *Dlx3*. IF at three and seven days post-infection revealed intense GFP signals in sockets and surrounding bone at three days (Supplementary Fig. 1d), substantially diminished by seven days (Supplementary Fig. 1e). Additionally, Western blot confirmed significant *Dlx3* downregulation in knockdown mice versus controls (Supplementary Fig. 1f), indicating that adenovirus infection and *Dlx3* suppression were successful.

Inhibition of *Dlx3* accelerated bone formation in extraction sockets

To evaluate the effect of *Dlx3* inhibition on bone formation in the extraction sockets, sagittal sections of the alveolar fossa were subjected to H&E staining at seven, nine, and fourteen days post-extraction. By days seven and nine, bone trabeculae formation was evident in the extraction sites of the *Dlx3*-knockdown mice, indicating enhanced osteogenesis. In contrast, control mice exhibited persistent inflammatory tissue infiltration (Fig. 1a—d, a'-d'). At 14 days, *Dlx3*-knockdown mice exhibited enhanced growth of bone trabeculae, while controls persisted with fibrous tissue and inflammation(Fig. 1e—f, e'-f'). To further assess the osteogenic capacity of the *Dlx3*-knockdown mice, RUNX2 immunohistochemical staining was performed at three and seven days post-extraction. The *Dlx3*-knockdown

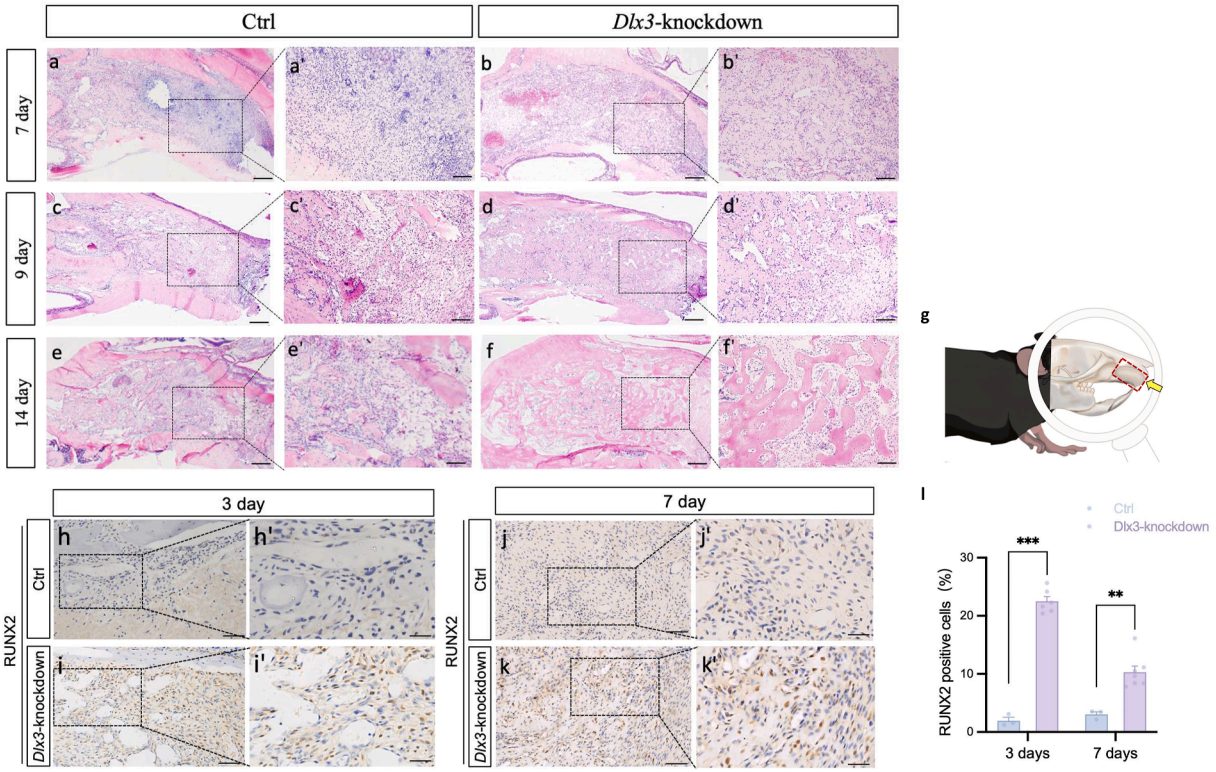

Figure 1 Earlier osteogenesis in extraction sockets of *Dlx3*-knockdown mice. **(a—f)** Sagittal images of H&E stained maxillary incisal alveolar fossae from *Dlx3*-knockdown and control mice at 7, 9, and 14 days after tooth extraction. Scale bars: 200 μm **(a'-f')** Higher magnification of the dashed boxes in (a—f), showing the anterior 1/3 of the extraction socket. Scale: 50 μm. **(g)** Diagram depicting sagittal plane sectioning of the post-extraction alveolar socket. **(h-k, h'-k')** IHC analysis demonstrated expression of runt-related transcription factor 2(RUNX2) protein in extraction sockets of Control and *Dlx3*-knockdown mice. Scale bars: (h—k): 50 μm; (h'-k'): 25 μm. **(l)** The ratio of RUNX2$^+$ cells per total cells, results were expressed as mean ± SD, $n = 3$. $^{**}P < 0.01$, $^{***}P < 0.001$. Ctrl, control; *Dlx3*, distal-less homeobox 3; RUNX2, runt-related transcription factor 2.

group exhibited a higher number of RUNX2-positive osteoblasts in the sockets (Fig. 1h—k, h'-k'). These findings suggest that short-term *Dlx3* inhibition accelerates early bone formation via osteoblast activation.

Inhibition of *Dlx3* in extraction sockets suppresses osteoclast activity

Osteoclasts were quantified via TRAP staining to determine the effects of *Dlx3* inhibition on osteoclastic activity. A significant reduction in osteoclast numbers was observed in the *Dlx3*-knockdown group at three, seven, and nine days post-extraction (Fig. 2). These findings suggest that *Dlx3* inhibition suppresses osteoclastic activity, reducing alveolar bone resorption.

Inhibition of *Dlx3* enhanced bone formation while preserving normal bone structure

Micro-computed tomography(Micro-CT) at three weeks post-extraction revealed enhanced bone formation in *Dlx3*-knockdown mice versus bone loss near the alveolar ridge in controls (Fig. 3a—d).The H&E staining corroborated these findings, showing that bone defect areas in the control group were predominantly filled with fibrous connective tissue (Fig. 3e—f, e'-f'). Quantitative analysis revealed significantly increased Tb.BV, BV/TV, Tb.BS, and Tb.N with decreased Tb.Sp in *Dlx3*-knockdown mice compared to the controls (Fig. 3g—k). These results suggest that short-term inhibition of *Dlx3* in the alveolar fossa promotes alveolar bone osteogenesis and increases bone density.

Inhibition of *Dlx3* in the alveolar socket suppressed *Thbs1* and elevated EMCN expression

To investigate key downstream regulators of osteogenic and osteoclastic activity after *Dlx3* inhibition, we performed RNA sequencing on alveolar bone.Transcriptome analysis revealed 135 significantly differentially expressed genes (DEGs) in *Dlx3*-knockdown mice, including 39 upregulated and 96 downregulated genes (fold change>2, $P < 0.05$; Fig. 4a).

Volcano plot and Kyoto Encyclopedia of Genes and Genomes (KEGG) pathway analysis of DEGs revealed significant enrichment in ECM-receptor interaction, focal adhesion, PI3K-Akt signaling, and TGF-β signaling pathways (Fig. 4a—e). Gene Ontology (GO) enrichment analysis further confirmed these findings (Supplementary Fig. 2). *Thbs1*, which encodes thrombospondin-1(THBS1),[24] was significantly downregulated and enriched across all key

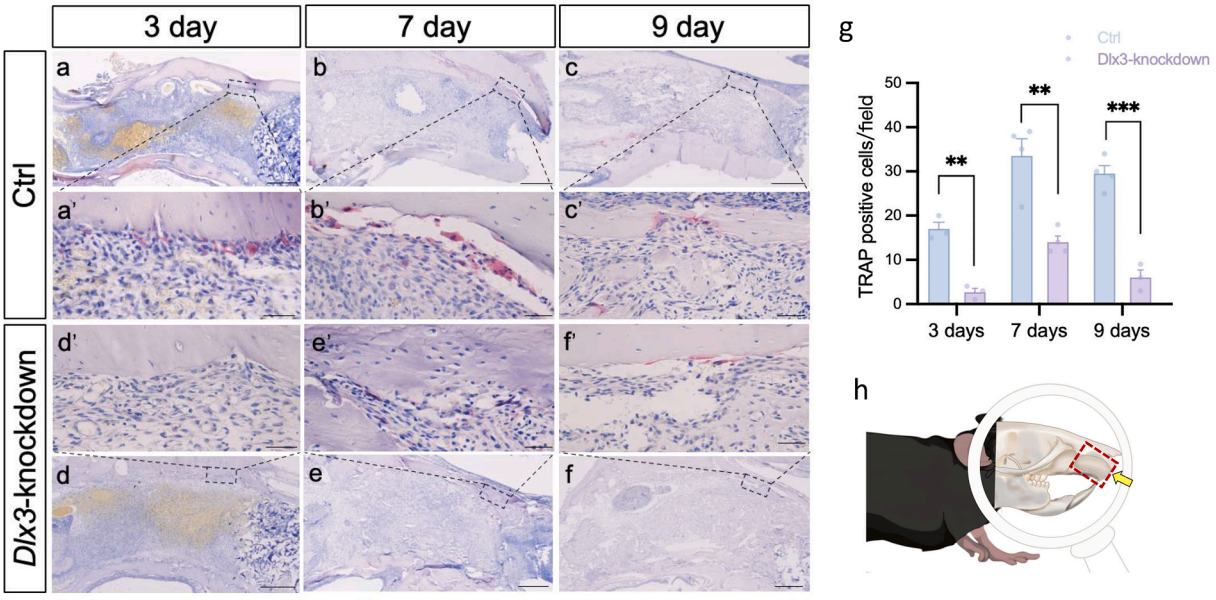

Figure 2 Decreased number of osteoclasts in extraction sockets of *Dlx3*-knockdown mice **(a—f)** Sagittal images of TRAP-stained maxillary incisal alveolar fossae from *Dlx3*-knockdown and control mice at 3,7, and 9 days after tooth extraction. Scale bars: 200 μm **(a'-f')** High magnification of TRAP staining in the anterior alveolar fossa near the cortical bone used for quantitative analysis. **(g)** Quantitative analysis of active osteoclasts. Active osteoclasts were defined as burgundy multinucleated cells along the ROI of the alveolar bone surface. n = 3 per group. *$P < 0.05$; **$P < 0.01$; ***$P < 0.001$. **(h)** Diagram depicting sagittal plane sectioning of the post-extraction alveolar socket. Ctrl, control; *Dlx3*, distal-less homeobox 3; TRAP, tartrate-resistant acid phosphatase.

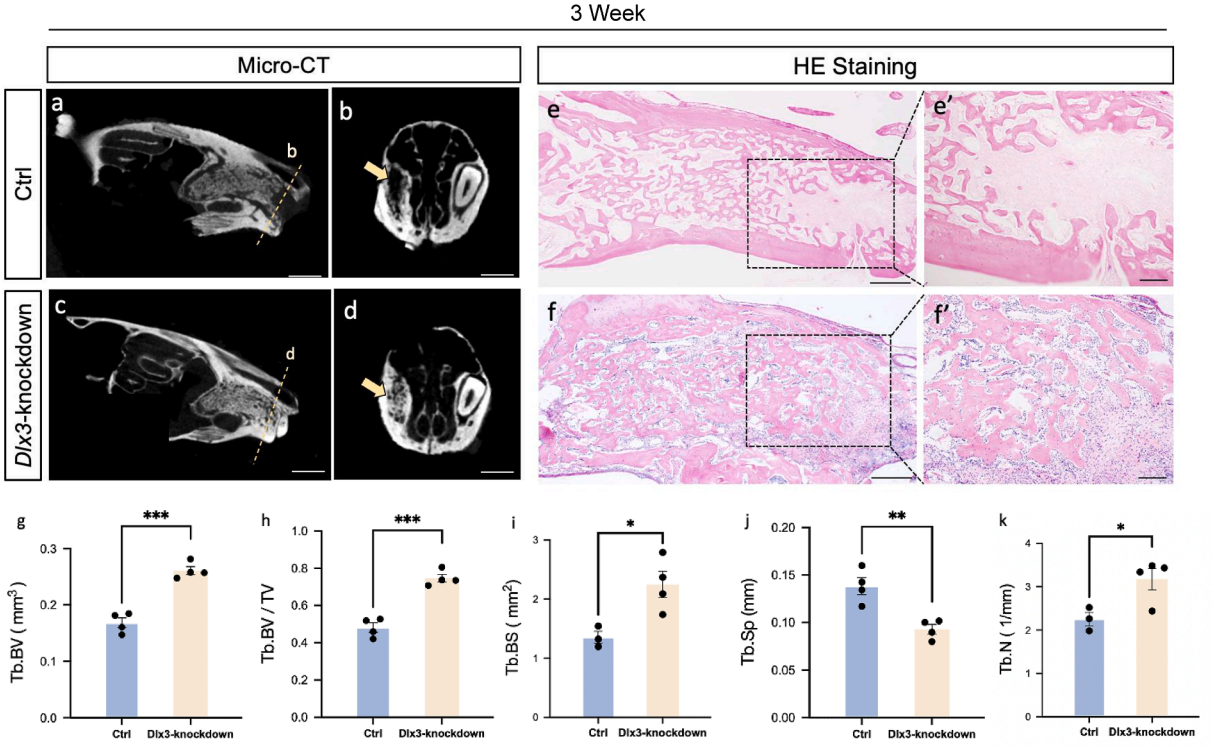

Figure 3 Increased osteogenesis in extraction sockets of *Dlx3*-knockdown mice. **(a, c)** Sagittal plane of Micro-CT images of maxillary incisor alveolar fossa from control and *Dlx3*-knockdown mice 3 weeks after tooth extraction. Scale bars: 2 mm. **(b, d)** Axial views of the anterior one-third of the extraction socket. Arrows indicate maxillary incisor alveolar fossa. Scale bars: 2 mm. **(e—f)** Sagittal images of H&E-stained maxillary incisal alveolar fossae from *Dlx3*-knockdown and control mice 3 weeks after tooth extraction. Scale bars: 200 μm. **(e'-f')** Higher magnification of the dashed boxes in (e—f), showing the anterior 1/3 of the extraction socket. Scale: 50 μm. **(g—k)** Bar graphs depicting trabecula bone volume (Tb. BV), bone volume to total volume ratio (BV/TV), trabecular bone surface (Tb. BS), trabecular separation (Tb. Sp), and trabecular number (Tb. N) in *Dlx3*-knockdown and control mice. n = 4 per group. Data were presented as mean ± SD. *$P < 0.05$; **$P < 0.01$; ***$P < 0.001$. Ctrl, control; *Dlx3*, distal-less homeobox 3.

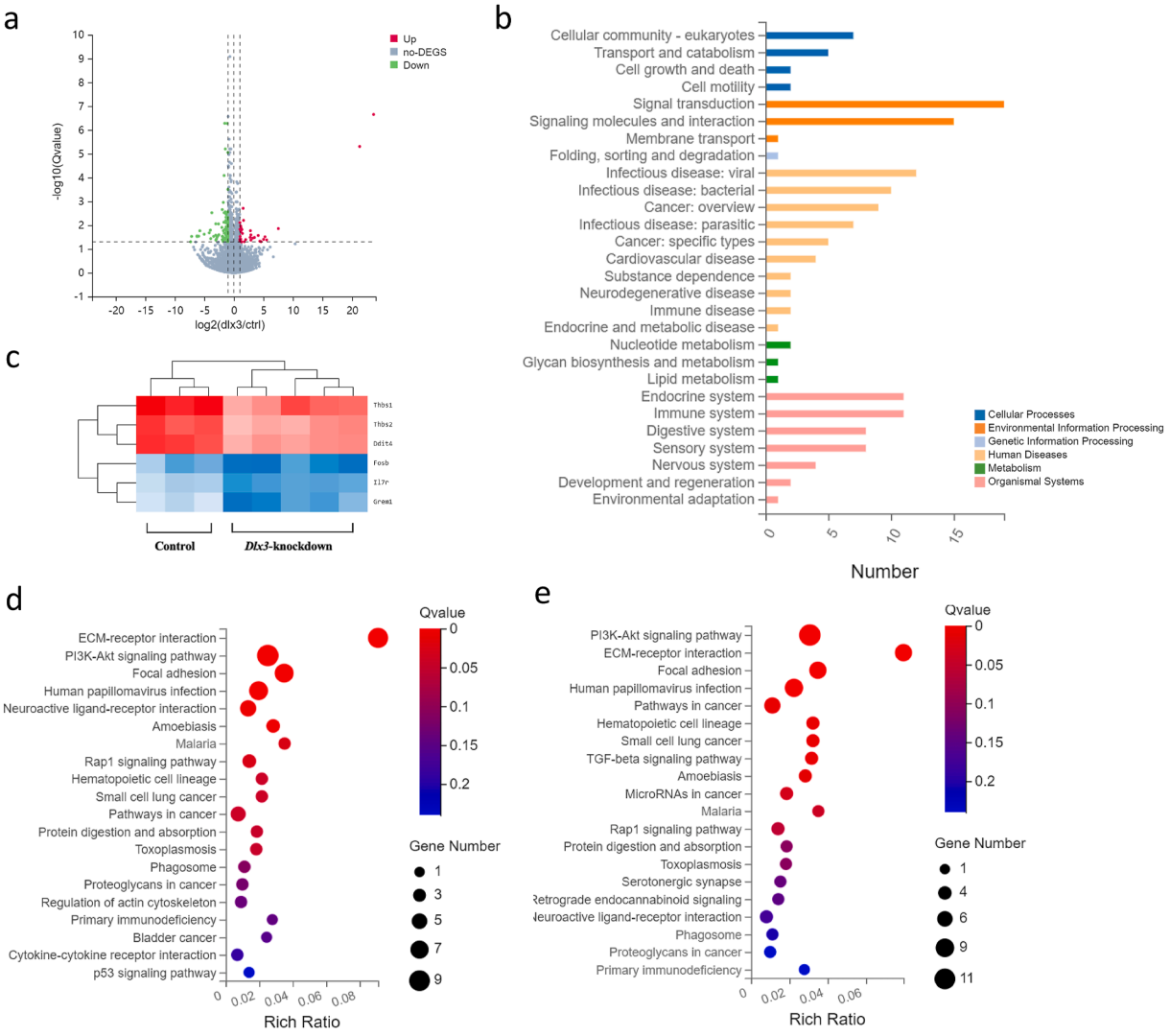

Figure 4 Gene function analysis of differentially expressed genes (DEGs). **(a)** Volcano plot of RNA sequencing showing the DEGs in extraction socket 5 days after tooth extraction from *Dlx3*-knockdown and control mice(n = 3). **(b)** KEGG pathway annotation, showing the summary of primary and secondary classification of KEGG pathways for DEGs.(c) Heatmap showing the relative expression levels of downstream molecules from Dlx3-knockdown and control mice. **(d—e)** Bubble maps of the KEGG pathway enrichment analysis for differentially expressed gene sets, including signal transduction, signaling molecules, and interaction. The size of the bubbles represents the number of differentially expressed genes, and the color shade depends on the adjusted *P*-value of each term. Ctrl, control; *Dlx3*, distal-less homeobox 3.

pathways.As a multifunctional regulator of cell adhesion, migration, and growth factor activity,[24,25] THBS1 suppression likely mediates enhanced socket healing. Heatmap analysis validated *Thbs1* downregulation (Fig. 4c).

IHC further confirmed these results, showing that the expression of THBS1 in the cytoplasm and interstitium of *Dlx3*-knockdown mice was downregulated at five days post-extraction compared to the control group (Fig. 5a—b, a'-b'). Subsequently, IF staining was performed to assess the expression intensity of Endomucin(EMCN) in extraction sockets at seven and nine days post-extraction. EMCN, a critical molecule involved in determining vascular type, is highly expressed in H-type vessels.[26,27] *Dlx3*-knockdown mice exhibited a significantly larger EMCN-positive area during early socket healing compared to control mice (Fig. 5c—k).

Adding THBS1 partially reversed the favorable phenotype of enhanced bone formation induced by local inhibition of *Dlx3*

To further investigate whether *Thbs1* acts as a downstream effector of *Dlx3* in promoting osteogenesis in extraction sockets, in vivo reversal experiments were performed. THBS1 was administered to *Dlx3*-knockdown mice sockets two days post-extraction (THBS1 group), while controls received normal saline (NS group). H&E staining showed

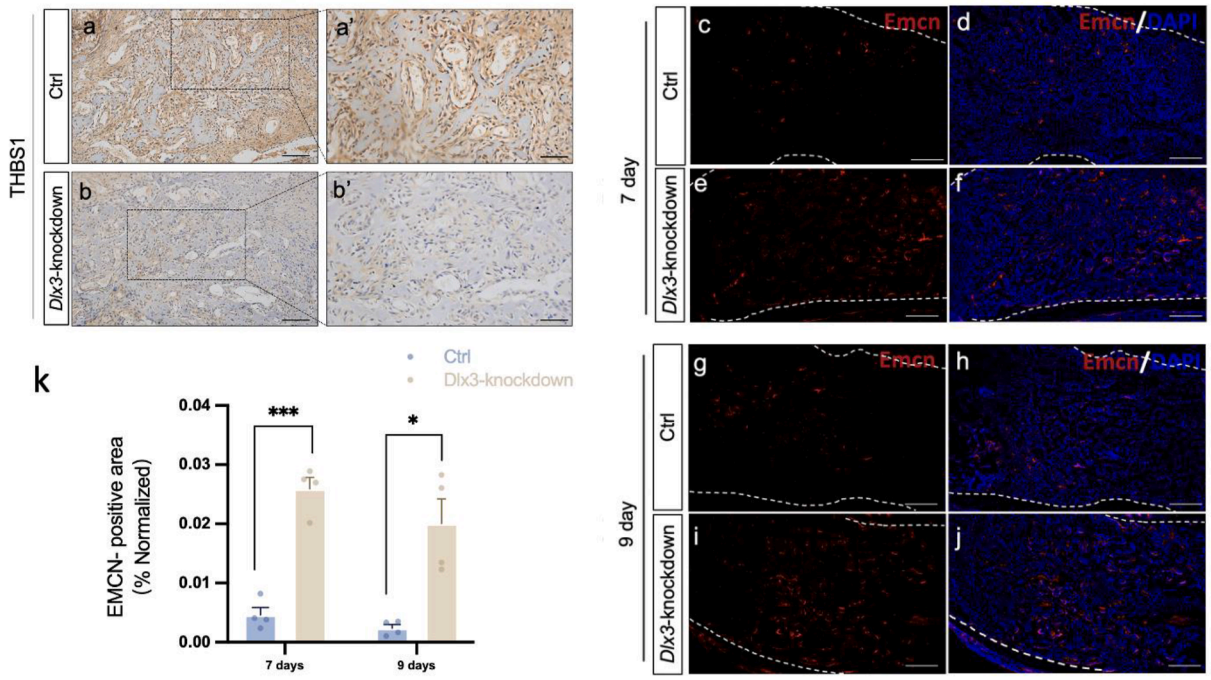

Figure 5 Reduced THBS1 and increased EMCN in extraction sockets of *Dlx3*-knockdown mice. **(a-b, a'-b')** IHC analysis showed the expression of THBS1 in extraction sockets of *Dlx3*-knockdown and control mice. Scale bars: (a—b):50 μm; (a'-b'): 25 μm. **(c—j)** Co-localization of EMCN (red) and DAPI (blue) showed the distribution of H-vessels in the extraction socket from *Dlx3*-knockdown and control mice at 7 and 9 days. The white dotted line outlined the outer contour of the alveolar fossa (boundary of the trabecular bone from the cortical bone). **(k)** Quantification analysis of the percentage of EMCN-positive area, results were expressed as mean ± SD, n = 4. $^{*}P < 0.05$, $^{***}P < 0.001$. Ctrl, control; *Dlx3*, distal-less homeobox 3; THBS1, thrombospondin 1; EMCN, Endomucin; DAPI, 4′,6-diamidino-2-phenylindole.

accelerated trabecular bone formation in NS compared to THBS1 mice (Fig. 6a—d, a'-d'). By 14 days post-extraction, NS group sockets were predominantly trabecular bone, whereas the THBS1 group exhibited areas largely occupied by fibrous connective tissue and inflammatory infiltrates (Fig. 6e—f, e'-f'). Micro-CT at three weeks revealed larger alveolar ridge defects in THBS1 mice (Fig. 6g—j), with significantly reduced Tb.BV and BV/TV (Fig. 6k—l). These data demonstrate that THBS1 upregulation partially reverses *Dlx3*-inhibition-enhanced osteogenesis.

Discussion

Maintaining alveolar bone mass remains a significant clinical challenge and a key focus of research. In this study, a mouse model of alveolar bone loss and healing was established. Enhanced bone formation and increased alveolar bone mass were observed in *Dlx3*-knockdown mice, which promoted osteogenesis through osteoblast activation and reduced bone resorption via osteoclast inhibition, all while preserving normal bone structure. RNA sequencing and subsequent analysis identified *Thbs1* as a critical downstream regulator.

Adenoviruses are widely used gene therapy vectors due to their high transduction efficiency, broad host tropism, and transient expression profile.[28,29] Unlike integrating viruses, they achieve peak expression rapidly without genomic integration.[30—32] In our study, viral effects were prominent at three days post-infection, with fluorescence signals becoming nearly undetectable by one week. This demonstrates that therapeutic efficacy requires early intervention and suggests minimal risk of long-term off-target effects.

Three weeks post-extraction, *Dlx3*-knockdown mice showed enhanced bone formation within the socket. Micro-CT analysis revealed significantly increased Tb.BV, BV/TV, and Tb.N compared to controls. These findings recapitulate the enhanced alveolar bone regeneration phenotype observed in TDO syndrome patients following *Dlx3* inhibition. H&E staining confirmed normal trabecular architecture in the alveolar socket—with no TDO-associated bone abnormalities.[26] Our results demonstrate that transient *Dlx3* suppression in extraction sockets drives bone mass accrual.

The role of *Dlx3* in bone remodeling remains controversial. While in vitro studies show *Dlx3* knockdown inhibits osteogenic differentiation,[33,34] deletion mutations paradoxically enhance osteogenesis by accelerating bone marrow stromal cell differentiation into osteoblasts.[23,35] Transgenic mice with a 4-bp *Dlx3* deletion further exhibit suppressed osteoclastogenesis.[23] In our model, *Dlx3*-knockdown mice showed increased Runx2^{+} osteoblasts and decreased osteoclasts during early post-extraction healing. This demonstrates that transient *Dlx3* inhibition in alveolar bone enhances osteogenesis through osteoblast activation while reducing resorption via osteoclast suppression—a dual mechanism explaining the increased socket bone density. These findings align with TDO syndrome patients

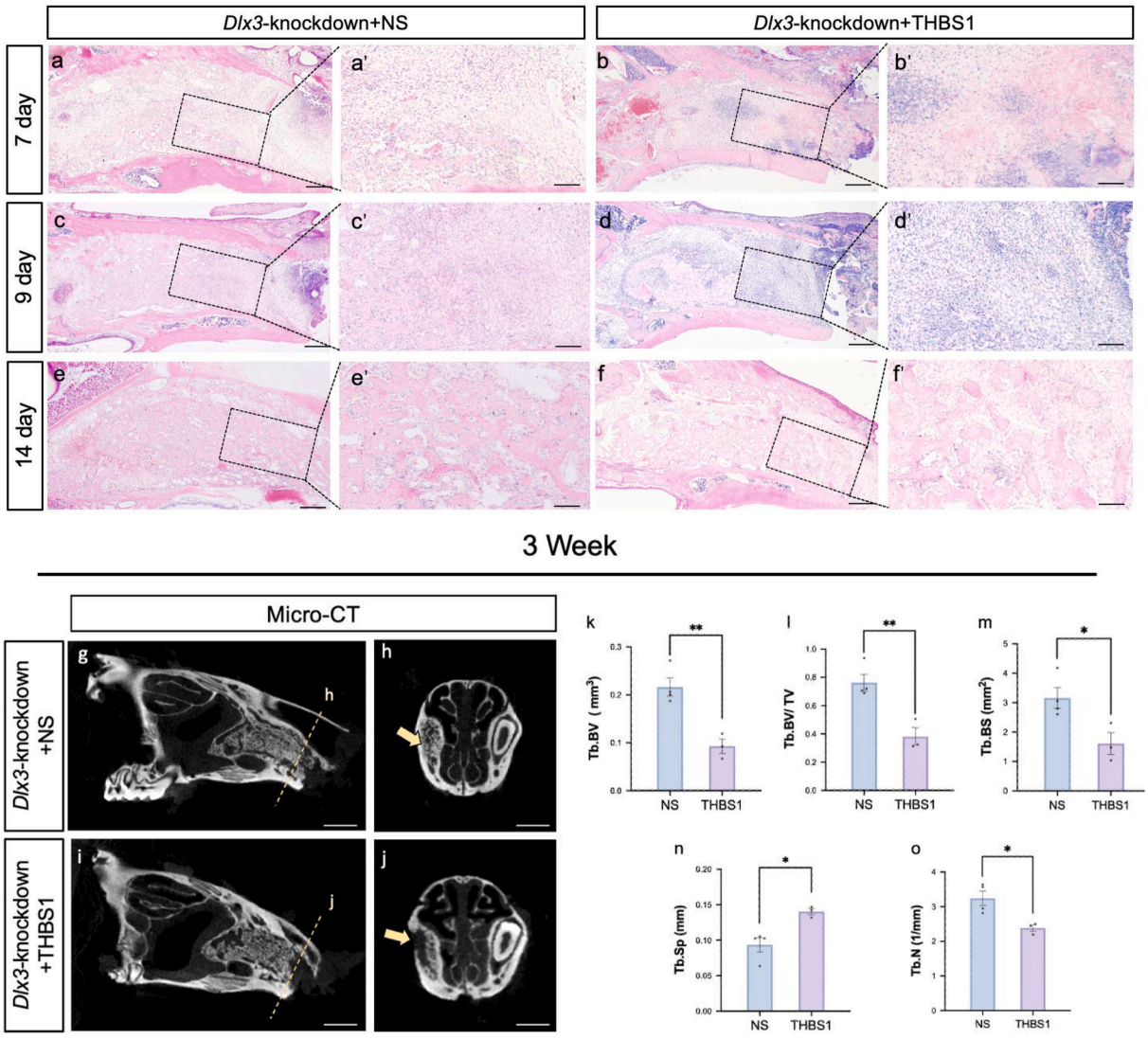

Figure 6 Adding THBS1 partially reversed the favorable phenotype of bone enhancement induced by local inhibition of *Dlx3*. **(a—f)** Sagittal images of H&E-stained maxillary incisal alveolar fossae from NS and THBS1 mice at 7,9, and 14 days after tooth extraction. Scale bars: 200 μm **(a'-f')** High magnification of the middle one-third of the extraction socket. **(g, i)** Sagittal plane of Micro-CT images of maxillary incisor alveolar fossa from NS and THBS1 mice 3 weeks after tooth extraction. Scale bars: 2 mm. **(h, j)** Axial views of the anterior 1/3 of the extraction socket. Arrows indicated maxillary incisor alveolar fossa. Scale bars: 2 mm. **(k-o)** Bar graphs depicting trabecula bone volume (Tb. BV), bone volume to total volume ratio (BV/TV), trabecular bone surface (Tb. BS), trabecular separation (Tb. Sp) and trabecular number (Tb. N) in *Dlx3*-knockdown and control mice. $n = 3$ per group. Data were presented as mean ± SD. ns not significant, $^{*}P < 0.05$, $^{**}P < 0.01$. Ctrl, control; *Dlx3*, distal-less homeobox 3; THBS1, thrombospondin 1; NS, normal saline.

and *DLX3* (Q178R)-transgenic mice,[20] confirming that localized short-term *Dlx3* suppression replicates pro-regenerative remodeling without genetic modification.

RNA sequencing and subsequent analysis revealed that *Thbs1* was significantly downregulated in the alveolar bone of *Dlx3*-knockdown mice five days post-extraction. Further reversal experiments demonstrated that adding *Thbs1* partially reversed the enhanced osteogenic phenotype induced by *Dlx3* inhibition, confirming it as a downstream target of *Dlx3*. *Thbs1* encodes THBS1, a multifunctional extracellular matrix and secreted protein.[24] THBS1 has been widely reported to play a critical role in angiogenesis and bone formation.[24] It may regulate alveolar bone remodeling through multiple mechanisms, including the inhibition of osteoblast-mediated bone mineralization and matrix production, as well as the suppression of osteogenic differentiation in mesenchymal stem cells via activation of latent TGF-β.[36,37]

THBS1 binding to CD36 and CD47 inhibits nitric oxide (NO) and cyclic guanosine monophosphate (cGMP) accumulation,[38] disrupting NO-mediated osteogenic-angiogenic coupling in bone repair.[39,40] H-type blood vessels, a specialized subset of capillaries in bone, play a critical role in angiogenesis and osteogenesis.[27] Yan et al. demonstrated spatially and functionally coupled formation of H-vessels with Runx2^{+} osteoprogenitor clusters in a mouse tooth

extraction model.[26] In our study, we assessed H-vessels in extraction sockets using EMCN—a specific marker for these vessels. *Dlx3*-knockdown mice showed increased H-vessels in early-healing sockets. We propose *Dlx3* suppression downregulates THBS1 to promote the coupling of H-type vessel formation and osteogenesis, enhancing bone maturation. Additional THBS1 mechanisms require further investigation.

In summary, the localized and temporary inhibition of *Dlx3* in the mouse alveolar socket following tooth extraction facilitates alveolar bone remodeling. This intervention has the potential to suppress osteoclast-mediated bone resorption while simultaneously enhancing new bone formation, ultimately promoting alveolar bone regeneration, without affecting the normal trabecular architecture. Consequently, *DLX3* is a promising therapeutic target for enhancing alveolar bone remodeling after tooth extraction.

Declaration of competing interest

The authors have no conflicts of interest relevant to this article.

Acknowledgments

This research was supported by the National Natural Science Foundation of China, grant numbers 82270944, 81900985 and 81600846.

Appendix A. Supplementary data

Supplementary data to this article can be found online at https://doi.org/10.1016/j.jds.2025.07.008.

References

1. Zhang Q, Yu Z, Wang Y, et al. Deproteinized bovine bone mineral with collagen for anterior maxillary ridge augmentation: a retrospective cohort study. *Clin Implant Dent Relat Res* 2025;27:e13433.
2. Haugen HJ, Lyngstadaas SP, Rossi F, Perale G. Bone grafts: which is the ideal biomaterial? *J Clin Periodontol* 2019;46:92—102.
3. Darby I, Chen S, De Poi R. Ridge preservation: what is it and when should it be considered. *Aust Dent J* 2008;53:11—21.
4. Chavda S, Levin L. Human studies of vertical and horizontal alveolar ridge augmentation comparing different types of bone graft materials: a systematic review. *J Oral Implantol* 2018;44:74—84.
5. Perić Kačarević Ž, Rider P, Alkildani S, et al. An introduction to bone tissue engineering. *Int J Artif Organs* 2020;43:69—86.
6. Yin Y, Shuai F, Liu X, Zhao Y, Han X, Zhao H. Biomaterials and therapeutic strategies designed for tooth extraction socket healing. *Biomaterials* 2025;316:122975.
7. Kimelman Bleich N, Kallai I, Lieberman JR, Schwarz EM, Pelled G, Gazit D. Gene therapy approaches to regenerating bone. *Adv Drug Deliv Rev* 2012;64:1320—30.
8. Evans CH. Gene therapy for bone healing. *Expet Rev Mol Med* 2010;12:e18.
9. Trombelli L, Farina R, Marzola A, Bozzi L, Liljenberg B, Lindhe J. Modeling and remodeling of human extraction sockets. *J Clin Periodontol* 2008;35:630—9.
10. Politis C, Schoenaers J, Jacobs R, Agbaje JO. Wound healing problems in the mouth. *Front Physiol* 2016;7:507.
11. Vieira AE, Repeke CE, Ferreira Junior SDB, et al. Intramembranous bone healing process subsequent to tooth extraction in mice: micro-computed tomography, histomorphometric and molecular characterization. *PLoS One* 2015;10:e0128021.
12. Liang B, Zhang W, Xue Y, et al. Observation and analysis of tooth extraction wound healing process of maxillary first molars in C57B/6 mice. *Chin J Pract Stomatol* 2019;12:46—50.
13. Feledy JA, Morasso MI, Jang SI, Sargent TD. Transcriptional activation by the homeodomain protein distal-less 3. *Nucleic Acids Res* 1999;27:764—70.
14. Hwang J, Kita R, Kwon HS, et al. Epidermal ablation of Dlx3 is linked to IL-17-associated skin inflammation. *Proc Natl Acad Sci U S A* 2011;108:11566—71.
15. Hwang J, Mehrani T, Millar SE, Morasso MI. Dlx3 is a crucial regulator of hair follicle differentiation and cycling. *Development* 2008;135:3149—59.
16. Choi SJ, Song IS, Feng JQ, et al. Mutant DLX3 disrupts odontoblast polarization and dentin formation. *Dev Biol* 2010;344:682—92.
17. Price JA, Wright JT, Kula K, Bowden DW, Hart TC. A common *DLX3* gene mutation is responsible for tricho-dento-osseous syndrome in Virginia and North Carolina families. *J Med Genet* 1998;35:825—8.
18. Li Y, Han D, Zhang H, et al. Morphological analyses and a novel de novo *DLX3* mutation associated with tricho-dento-osseous syndrome in a Chinese family. *Eur J Oral Sci* 2015;123:228—34.
19. Liu H, Wang Y, Liu H, et al. Novel *DLX3* variant identified in a family with tricho-dento-osseous syndrome. *Arch Oral Biol* 2022;141:105479.
20. Zhao N, Han D, Liu H, et al. Senescence: novel insight into *DLX3* mutations leading to enhanced bone formation in Tricho-Dento-Osseous syndrome. *Sci Rep* 2016;6:38680.
21. Morasso MI, Grinberg A, Robinson G, Sargent TD, Mahon KA. Placental failure in mice lacking the homeobox gene *Dlx3*. *Proc Natl Acad Sci U S A* 1999;96:162—7.
22. Clark PA, Brown JL, Li S, et al. Distal-less 3 haploinsufficiency results in elevated placental oxidative stress and altered fetal growth kinetics in the mouse. *Placenta* 2012;33:830—8.
23. Choi SJ, Roodman GD, Feng JQ, et al. In vivo impact of a 4 bp deletion mutation in the *DLX3* gene on bone development. *Dev Biol* 2009;325:129—37.
24. Adams JC, Lawler J. The thrombospondins. *Cold Spring Harbor Perspect Biol* 2011;3:a009712.
25. Isenberg JS, Roberts DD. THBS1 (thrombospondin-1). *Atlas Genet Cytogenet Oncol Haematol* 2020;24:291—9.
26. Yan ZQ, Wang XK, Zhou Y, et al. H-type blood vessels participate in alveolar bone remodeling during murine tooth extraction healing. *Oral Dis* 2020;26:998—1009.
27. Kusumbe AP, Ramasamy SK, Adams RH. Couplin of angiogenesis and osteogenesis by a specific vessel subtype in bone. *Nature* 2014;507:323—8.
28. Lundstrom K. Viral vectors in gene therapy. *Diseases* 2018;6:42.
29. Young LS, Searle PF, Onion D, Mautner V. Viral gene therapy strategies: from basic science to clinical application. *J Pathol* 2006;208:299—318.
30. Crystal RG. Adenovirus: the first effective in vivo gene delivery vector. *Hum Gene Ther* 2014;25:3—11.
31. Dunn CA, Jin Q, Taba MJ, Franceschi RT, Bruce RR, Giannobile WV. BMP gene delivery for alveolar bone engineering at dental implant defects. *Mol Ther* 2005;11:294—9.
32. Zhang Y, Huang J, Wang C, et al. Application of HIF-1α by gene therapy enhances angiogenesis and osteogenesis in alveolar bone defect regeneration. *J Gene Med* 2016;18:57—64.

33. Li J, Lin Q, Lin Y, Lai R, Zhang W. Effects of *DLX3* on the osteogenic differentiation of induced pluripotent stem cell-derived mesenchymal stem cells. *Mol Med Rep* 2021;23:232.
34. Li D, Yuan Q, Xiong L, Li A, Xia Y. The miR-4739/DLX3 axis modulates bone marrow-derived mesenchymal stem cell (BMSC) osteogenesis affecting osteoporosis progression. *Front Endocrinol* 2021;12:703167.
35. Choi SJ, Song IS, Ryu OH, et al. A 4 bp deletion mutation in DLX3 enhances osteoblastic differentiation and bone formation in vitro. *Bone* 2008;42:162—71.
36. Ueno A, Miwa Y, Miyoshi K, et al. Constitutive expression of thrombospondin 1 in MC3T3-E1 osteoblastic cells inhibits mineralization. *J Cell Physiol* 2006;209:322—32.
37. Bailey DuBose K, Zayzafoon M, Murphy-Ullrich JE. Thrombospondin-1 inhibits osteogenic differentiation of human mesenchymal stem cells through latent TGF-β activation. *Biochem Biophys Res Commun* 2012;422:488—93.
38. Koduru SV, Sun B, Walker JM, et al. The contribution of cross-talk between the cell-surface proteins CD36 and CD47—TSP-1 in osteoclast formation and function. *J Biol Chem* 2018;293:15055—69.
39. Amend SR, Uluckan O, Hurchla M, et al. Thrombospondin-1 regulates bone homeostasis through effects on bone matrix integrity and nitric oxide signaling in osteoclasts. *J Bone Miner Res* 2015;30:106—15.
40. Isenberg JS, Martin-Manso G, Maxhimer JB, Roberts DD. Regulation of nitric oxide signalling by thrombospondin 1: implications for anti-angiogenic therapies. *Nat Rev Cancer* 2009;9:182—94.